JACS Au
AN OPEN ACCESS JOURNAL OF THE AMERICAN CHEMICAL SOCIETY

pubs.acs.org/jacsau
Letter

Mechanism of Methylene Blue Inducing the Disulfide Bond Formation of Tubulin-Associated Unit Proteins

Dong-Hyun Seo, Yang Hoon Huh, Hae-Kap Cheong, Eun-Hee Kim, Jong-Soo Lim, Min Jung Lee, Donghan Lee,* and Kyoung-Seok Ryu*

Cite This: JACS Au 2024, 4, 2451−2455

ABSTRACT: Methylene blue (MB) has recently completed a Phase-3 clinical trial as leuco-methylthioninium (LMT) bis-(hydromethanesulfonate) for treating Alzheimer's disease. Herein, we investigated the mechanism underlying the MB inhibition of tubulin-associated unit (tau) aggregation by focusing on tau monomers. We found that MB causes disulfide bond formation, resulting in strong nuclear magnetic resonance chemical shift perturbations in a large area of tau proteins. The oxidized form of MB, namely methylthioninium (MT^+), specifically catalyzed the oxidation of cysteine residues in tau proteins to form disulfide bonds directly using O_2. This process is independent of the MT^+-to-LMT redox cycle. Moreover, MT^+ preferentially oxidized C291 and C322 in the lysine-rich R2 and R3 domains. Under *in vivo* brain physoxia conditions, LMT may convert to MT^+, possibly interfering with tau fibrillation via disulfide bond formation.

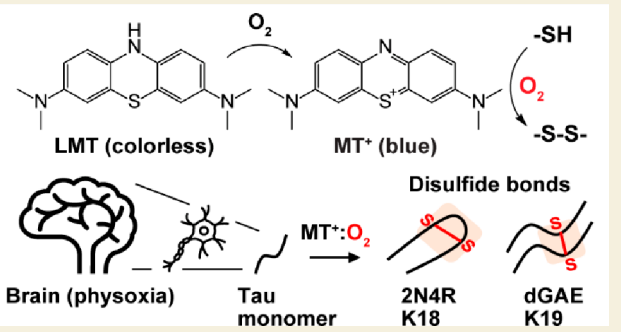

KEYWORDS: *methylene blue, methylthioninium, cysteine oxidation, tau aggregation inhibitor, nuclear magnetic resonance, oxygen*

INTRODUCTION

Presently, tubulin-associated unit (tau) aggregation inhibitors are being developed as novel therapeutic agents for treating Alzheimer's disease. Among them, methylene blue (MB), a phenothiazine derivative, belonging to the category of direct aggregation inhibitors, is one of the leading candidate therapeutics.[1,2] MB exhibits low dose-dependent toxicity and is presently used for treating methemoglobinemia.[3] MB generally exists in two different oxidation states: (i) the oxidized form, namely, methylthioninium (MT^+), with a strong blue color; and (ii) the colorless reduced form, namely, leucomethylthioninium (LMT), due to the breaking of aromaticity and loss of the planar structure. Because red blood cells absorb LMT more efficiently than MT^+,[4] its reduced form is stabilized by two mesylate ions (LMT bis-hydromethanesulfonate [LMTM]). LMTM has just completed a Phase-3 clinical trial for treating Alzheimer's disease and frontotemporal dementia (November 2022, TauRx Pharmaceuticals).

Despite many studies on the effects of MB on tau aggregation and disaggregation processes,[2,5] the detailed mechanism underlying MB interaction with the tau monomer is still unclear. Reportedly, MB (particularly the LMT form) specifically binds the regions of the full-length tau (2N4R), including C291 and C322, and inhibits tau aggregations through various cysteine (Cys) oxidations, including sulfenic, sulfinic, and sulfonic acids.[6] Moreover, molecular dynamics simulations proposed that MT^+ can interact with two critical regions of fibril-forming sequences (namely, V275-K280 and V306-K311) near the Cys residues.[7] Nevertheless, the detailed mechanism of MB interacting with the tau monomer according to the specific redox states remains unelucidated. Notably, MT^+ and LMT may interact with tau monomers in fundamentally different ways due to their distinct chemical structures, particularly in terms of aromaticity.

Herein, the specific effects of MT^+ and LMT on tau interactions were investigated in an O_2-controlled environment, as LMT quickly converts to MT^+ due to air oxidation. We identified that MB-driven Cys oxidation leading to disulfide bond formation is not caused by the direct association of MB with tau monomers but by the catalytic action of MT^+ rather than LMT using O_2 molecules. Additionally, we confirmed that C291 and C322, located in repeat domains 2 and 3 (R2 and R3), respectively, are highly susceptible to MT^+-driven Cys oxidation to disulfide bonds.

Received: March 26, 2024
Revised: April 22, 2024
Accepted: April 24, 2024
Published: May 7, 2024

https://doi.org/10.1021/jacsau.4c00262
JACS Au 2024, 4, 2451−2455

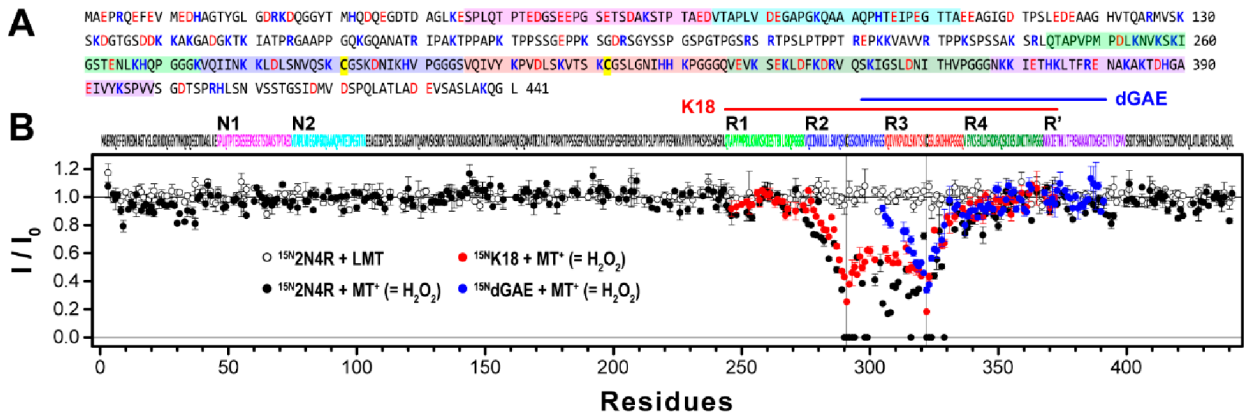

Figure 1. MB-induced chemical shift perturbations (CSPs) of ^{15N}2N4R, ^{15N}K18, and ^{15N}dGAE. (A) Amino acid sequence of 2N4R. N1, N2, four repeats (R1−R4), and R′ domains are indicated with different colored boxes. Positively and negatively charged residues are indicated with blue and red color, respectively. (B) Sizes of K18 and dGAE are indicated on the top. HSQC peak intensities of ^{15N}2N4R, ^{15N}K18, and ^{15N}dGAE in the presence of 1 mM MT$^+$, compared with those of the native (reduced) ones. In the presence of 1 mM LMT, peak intensities of ^{15N}2N4R were not changed. Locations of C291 and C322 are indicated using vertical lines.

RESULTS AND DISCUSSION

MB Does Not Directly Bind to Tau Monomer but Causes Oxidations of the Cys Residues

We investigated the direct interactions between MB and 2N4R using two different forms of MB (MT$^+$ and LMT). MT$^+$ led to the disappearance of many peaks in the C291 and C322 regions, resulting in an identical ^{1}H−^{15}N heteronuclear single quantum coherence (HSQC) spectrum of ^{15N}2N4R to that of a previous study believed to have been conducted with LMT.[6] However, the HSQC spectrum was unaffected by LMT (Figures 1B and S1A). Interestingly, occasional vortexing of the nuclear magnetic resonance (NMR) tube changed the colorless LMT to blue within a few hours, even in the presence of 1 mM dithiothreitol (DTT), resulting in the same spectrum of ^{15N}2N4R as that obtained by MT$^+$. Because the results contradicted the previous belief that MB forms a stable complex with the tau monomer, resulting in Cys oxidation,[6,7] and implied an alternative mechanism underlying MB-mediated Cys oxidation, we examined it with other oxidation methods, such as H_2O_2. The ^{1}H−^{15}N HSQC spectra of ^{15N}2N4R incubated with H_2O_2 and MT$^+$ were identical (Figure 1B and S1A). The shorter form of tau, namely, ^{15N}K18 (Figure S1C) and ^{15N}dGAE (Figure S1D) yielded similar results. Although the peak intensities around the Cys residues were notably reduced, the peaks did not disappear completely, likely because of their smaller size compared with that of 2N4R (Figure 1B). Therefore, the spectral changes affecting >60 residues of ^{15N}2N4R were solely due to Cys oxidation and not direct interactions between tau monomers and MB.

It has also been reported that the HSQC spectra of ^{15N}2N4R in the presence of the N-demethylated MB derivatives (namely azure A and B) show considerable changes in the N-terminal part (residues 1−130) and R′ domain, in addition to the four repeat domains (R1−R4) contrast to MB.[6] Although similar changes in the presence of azure A have been observed, the previous results for azure B were not be reproduced. A simple explanation is that azure A and B do not bind directly to tau, but there may be an unidentified source, such as a metal ion in azure A. The HSQC changes in the presence of azure A completely disappeared by adding ethylenediaminetetraacetic acid (Figure S2). Moreover, the HSQC spectrum in the presence of azure A was similar to that obtained in the presence of Zn^{2+} (Figure S2). Because the Zn^{2+}-binding sites of ^{15N}2N4R have been recently determined,[8] additional chemical shift perturbations (CSPs) could be induced by Zn^{2+} from an unknown manufacturing source, not by azure A.

Cysteine States in Tau Proteins Induced by MT$^+$-Mediated Oxidation

To clarify the Cys oxidation states by molecular size and the $^{13}C_\beta$-chemical shift (CS) of the Cys residue, we first selected a dGAE containing only one Cys residue (C322) to reduce the complexity. After oxidizing dGAE, the molecular weight was analyzed using size-exclusion chromatography multiangle light scattering (SEC-MALS) (Figure 2A), which confirmed that the

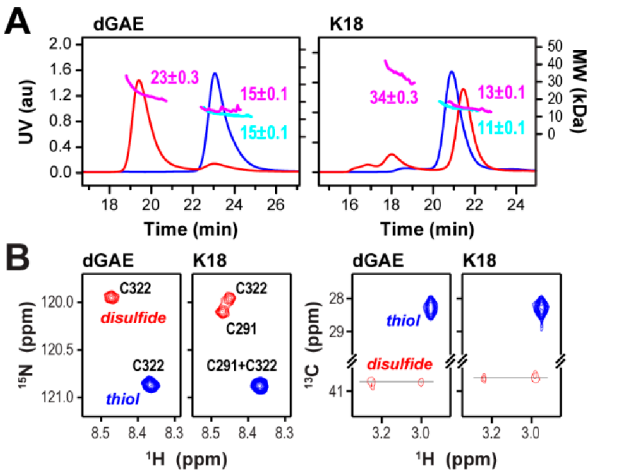

Figure 2. Characterizations of the Cys oxidation states in tau proteins. (A) dGAE (top) and K18 (bottom) proteins (5 mg/mL) were incubated in the presence of 5 mM dithiothreitol (blue) or 5 mM H_2O_2 (red) for 30 min at room temperature, and then SEC-MALS analyses were performed. Absolute molecular weights (MWs) were measured via the online MALS analyses. Calculated MWs of the monomers are as follows: dGAE, 10296.8; K18, 13813.9 g/mol. (B) ^{1}H−^{15}N and ^{1}H−^{13}C HSQC spectra of $^{13C/15N}$Cys−dGAE and $^{13C/15N}$Cys−K18 were recorded in the reduced (blue) and oxidized (red) states, respectively. Intensities of ^{1}H−^{15}N and ^{1}H−^{13}C HSQC peaks decreased to approximately 50% and 10%, respectively, compared with those of the reduced forms.

https://doi.org/10.1021/jacsau.4c00262
JACS Au 2024, 4, 2451−2455

oxidized dGAE primarily existed as a dimer, possibly by forming an intermolecular disulfide bond (interDS) via C322 ($dGAE^{interDS}$). Furthermore, the $^{13}C_{\beta}$-CS of $^{13C/15N}$Cys-specific labeled $dGAE^{interDS}$ (40.7 ppm) was in line with that of the predicted CS (40.1 ppm) (Figure S3; Supplementary Text). Regarding K18, we found that oxidized K18 mostly existed as a monomer through SEC-MALS analysis (Figure 2A), but the $^{13}C_{\beta}$-CSs of $^{13C/15N}$Cys-K18 were similar to that of $dGAE^{interDS}$ (Figure 2B). Hence, we concluded that the oxidized state of the Cys residues in K18 was the intramolecular DS between C291 and C322 ($K18^{intraDS}$).

MB could preferentially act on the Cys residues in the tau repeat domains (R1 and R4) that exhibit a high lysine (Lys) population (Figure 1A). We estimated the effect of a high Lys population on the oxidation of C291 and C322 in R2 and R3, respectively, by using two different 2N4R (S56C and I354C) mutant proteins in which S56 and I354 were in the N1 (less Lys) and R4 (high Lys) domains, respectively (Figure 1A). The time-coursed $^{1}H-^{15}N$ HSQC spectra of ^{15N}2N4R mutant proteins showed that MT^{+} oxidized all Cys residues, even at much lower molar equivalents, and the oxidation of C291, C322, and C354 was faster than that of C56 (Figure 3 and Figure S4). Although the exact reason for this is unknown, cation−pi interactions between the Lys residues and aromatic MT^{+} may be the reason.[9]

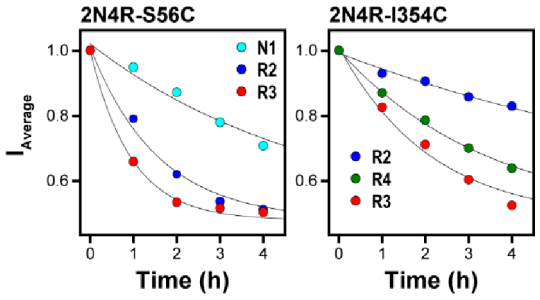

Figure 3. Oxidation rates of each Cys residue by MT^{+}. Decreasing intensities result from the disulfide bond formation of ^{15N}2N4R (S56C, N1; C291, R2; C322, R3; and I354C, R4). Time-coursed $^{1}H-^{15}N$ HSQC spectra of 0.1 mM ^{15N}2N4R-S56C (left) and ^{15N}2N4R-I354C (right) in the presence of 50 and 10 μM MT^{+}, respectively, were recorded at 10 °C. Averaged intensities ($I_{Average}$) of the region for each Cys (±15 residues) are plotted for increasing incubation times.

MT^{+}-Mediated Cys Oxidation Is Independent of the Redox Cycle of MB

To elucidate the mechanism of Cys oxidation, we focused on the color of the NMR samples and the $^{1}H-^{15}N$ HSQC spectra of K18 following MT^{+} addition. If the redox cycle of MB is directly related to Cys oxidation (Figure 4A), then changes in the $^{1}H-^{15}N$ HSQC spectra would be accompanied by a color change from blue to transparent (MT^{+} to LMT). However, no color changes were detected when the spectra showed changes (data not shown). Reportedly, aminothienopyridazines induce the disulfide bonding of K18 using O_2 rather than H_2O_2, which is the byproduct of the redox reaction of the dye.[10,11] Thus, the MT^{+}-induced disulfide bonding could occur through O_2, as the concentration of O_2 dissolved in a buffer varies from 0.35 to 0.2 mM based on temperatures ranging from 10 to 40 °C.[12] O_2 in air (approximately 21%), corresponding to approximately 10 mM, can supply more O_2 to the NMR sample. To test the

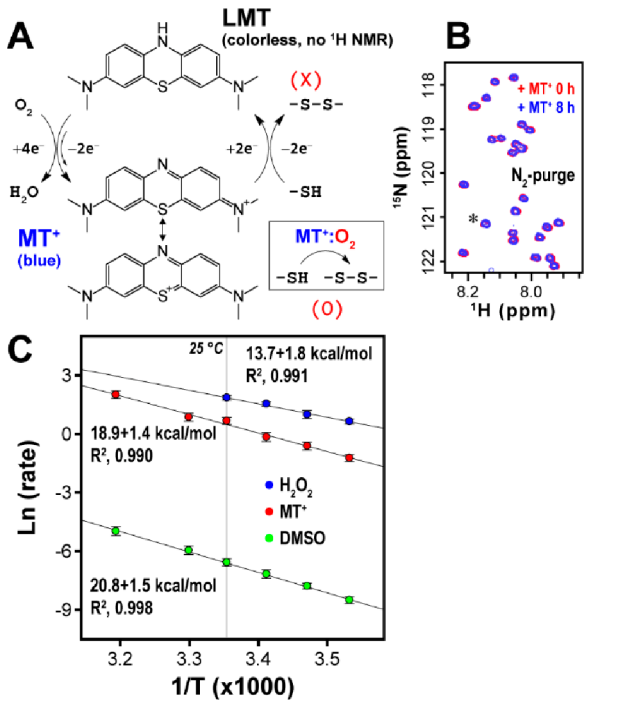

Figure 4. Oxidation of Cys by MT^{+} is dependent on the dissolved O_2 in the solution. (A) Redox cycle of MB. Sequestering in the MT^{+} state does not allow Cys oxidation, either directly by coupling to the redox cycle of MB or indirectly by the H_2O_2 byproduct. (B) NMR sample of 0.1 mM ^{15N}K18 and 0.5 mM MT^{+} was degassed and prepared under N_2 gas. $^{1}H-^{15}N$ heteronuclear single quantum coherence spectrum was not changed at least for 8 h. (C) Arrhenius plots for the oxidation rates of *N*-acetyl Cys (NAC) by H_2O_2, MT^{+}, and dimethyl sulfoxide (DMSO). Values of k_{H2O2}, $k_{MT+}\cdot[O_2]$, and k_{DMSO} are 6.38, 1.96, and 1.40×10^{-3} $M^{-1}\cdot min^{-1}$, respectively, at 25 °C.

effect of the oxidation of O_2 during MT^{+}-mediated oxidation in the NMR tube, we prepared a degassed ^{15N}K18 solution and mixed it with MT^{+} in an N_2 chamber, where the O_2 content was maintained below 0.6%. Notably, MT^{+} under the depleted O_2 conditions did not efficiently oxidize the Cys residues of K18 (Figure 4B). Therefore, MT^{+}-catalyzed Cys oxidation was concluded to be independent of the MB redox cycle.

MT^{+} Catalyzes Cys Oxidation by Utilizing O_2

We attempted to elucidate the detailed mechanism underlying MT^{+}-mediated Cys oxidation using N-acetyl Cys (NAC) as a model compound. LMT is quickly oxidized to MT^{+} in the presence of air, as demonstrated by the blue bottle experiment.[13] However, the MT^{+} state was maintained for at least overnight in the presence of 5 mM NAC, and even at the air interface, it remained stable in the presence of 5 mM DTT (Figure S5B and C). The end product of NAC oxidation was confirmed to be a disulfide-bonded NAC dimer through diffusion-ordered spectroscopy (NMR) (Figure S6A). Interestingly, the addition of 1 mM NAC considerably broadened the ^{1}H-peaks of MT^{+} while preserving the intense blue color of the solution. Because there were no corresponding changes in the ^{1}H-peaks of NAC, it was concluded that NAC did not directly interact with MT^{+} (Figure S6C). Because the presence of NAC in the solution possibly depleted dissolved O_2, we tested if the peak broadening of MT^{+} was dependent on the exchange process with O_2. The incubation of partially oxidized LMTM (a mixture of LMT and MT^{+}) in the air gradually increased the height of the methyl peak while decreasing the

https://doi.org/10.1021/jacsau.4c00262
JACS Au 2024, 4, 2451−2455

peak width. Moreover, the O_2-depletion (N_2 purging) in the NMR tube broadened the methyl peak of MT^+ even in the absence of NAC (Figure S6E). Possibly, MT^+ interacts directly with O_2 in solution, and the peak broadening may be dependent on the O_2 concentration.

The activation energies (E_a's) for NAC oxidation driven by MT^+, dimethyl sulfoxide (DMSO), and H_2O_2 were determined. The detailed derivations of the rate constants for each case are described in the Supplementary Text (Scheme S1). The air oxidation rates at different temperatures were subtracted (Table S1A). The rate constant of the NAC oxidation driven by MT^+ ($k_{MT+\cdot}[O_2]$, 1.96 $M^{-1}\cdot min^{-1}$) was much higher than that by DMSO (k_{DMSO}, 1.40 × 10^{-3} $M^{-1}\cdot min^{-1}$) at 25 °C (Table S1B). The E_a's of MT^+, DMSO, and H_2O_2 were 18.9 ± 1.4, 20.8 ± 1.5, and 13.7 ± 1.8 kcal/mol, respectively (Figure 4C), which indicates the MT^+-induced oxidation is more effective than the O_2 oxidation alone at high temperatures, particularly at physiological temperature.

Although LMT can also inhibit tau aggregation in a Cys-independent manner, likely through interaction with oligomers or fibrils,[14] we confirmed that MT^+-driven $dGAE^{interDS}$ and $K18^{intraDS}$ specifically interfered with tau aggregation (Figure S7; Supplementary Text). InterDS enhance and suppress the aggregation of K19 and dGAE, respectively, which seem to depend on the position of the Cys residue in fibrils (C291 in the fuzzy coat; C322 in the core).[15] Although the intraDS of K18 primarily suppresses aggregation,[10] reportedly, long incubation induces fibrils of $2N4R^{intraDS}$ that are less stable than those of 2N4R. These fibrils are effective for seeding $2N4R^{intraDS}$ monomers and can be disaggregated via Cys reduction, suggesting a thiol-based intramolecular redox switching mechanism.[16]

CONCLUSION

Much attention has been paid to the redox state of MB with regard to its medicinal activity. Herein, we report another mechanism by which MT^+, not LMT, induces disulfide bond formation in tau proteins by catalyzing O_2, which is associated with tau aggregation inhibition. Furthermore, our findings show that MT^+-mediated Cys oxidation is more effective than O_2 oxidation alone, particularly at physiological temperatures. Because lipophilic LMT can diffuse across the membrane and can be sequestered within the cells by reoxidization,[17] most LMT likely converts to MT^+ under the *in vivo* equivalent of the physoxia (3.0−7.4% O_2) condition,[18] acting as a tau aggregation inhibitor by inducing the disulfide bonds. The C291 and C322 residues of the tau protein in the Lys-rich R2 and R3 domains exhibited a higher susceptibility to oxidization. Altogether, the *in vivo* O_2 level may be an important factor in the disulfide bond formation of the tau protein by MT^+. In addition, direct interaction of MT^+ with O_2 may correlate with a previous study showing that MB increases brain oxygen consumption and facilitates memory retention in rats in a dose-dependent manner.[19]

ASSOCIATED CONTENT

Supporting Information

The Supporting Information is available free of charge at https://pubs.acs.org/doi/10.1021/jacsau.4c00262.

Materials, detailed experimental procedures, kinetics tables of NAC oxidation, NMR spectra of tau proteins, detailed characterization of MT^+-mediated Cys oxidation, and aggregation assays of tau proteins (PDF)

AUTHOR INFORMATION

Corresponding Authors

Donghan Lee − *Ochang center, Korea Basic Science Institute, Cheongju-Si, Chungcheongbuk-Do 28119, South Korea*; Phone: +82-43-240-5073; Email: dlee04@kbsi.re.kr

Kyoung-Seok Ryu − *Ochang center, Korea Basic Science Institute, Cheongju-Si, Chungcheongbuk-Do 28119, South Korea; KBSI School of Bioscience, University of Science and Technology, Cheongju-Si, Chungcheongbuk-Do 28119, South Korea*; orcid.org/0000-0002-8422-6669; Phone: +82-43-240-5064; Email: ksryu@kbsi.re.kr

Authors

Dong-Hyun Seo − *Ochang center, Korea Basic Science Institute, Cheongju-Si, Chungcheongbuk-Do 28119, South Korea; KBSI School of Bioscience, University of Science and Technology, Cheongju-Si, Chungcheongbuk-Do 28119, South Korea*

Yang Hoon Huh − *Ochang center, Korea Basic Science Institute, Cheongju-Si, Chungcheongbuk-Do 28119, South Korea*

Hae-Kap Cheong − *Ochang center, Korea Basic Science Institute, Cheongju-Si, Chungcheongbuk-Do 28119, South Korea*

Eun-Hee Kim − *Ochang center, Korea Basic Science Institute, Cheongju-Si, Chungcheongbuk-Do 28119, South Korea*

Jong-Soo Lim − *Novorex Inc., Seongnam-Si, Gyeonggi-Do 13493, South Korea*

Min Jung Lee − *Dong-A ST Research Institute, Yongin-Si, Gyeonggi-Do 17073, South Korea*

Complete contact information is available at: https://pubs.acs.org/10.1021/jacsau.4c00262

Author Contributions

J.S.L., M.J.L,. and K.S.R. organized the project. D.L. and K.S.R. designed experiments and wrote the manuscript. D.H.S. performed main experiments including analyses. D.H.S. and K.S.R. analyzed the data and prepared figures. Y.H.H., H.K.C., and E.H.K performed additional experiments.

Notes

The authors declare no competing financial interest.

ACKNOWLEDGMENTS

We are very grateful to Prof. Dr. M. Zweckstetter (Max Planck Institute for Biophysical Chemistry) for providing the $^1H-^{15}N$ HSQC chemical shifts of $^{15N}2N4R$. This work was supported by the KBSI grants (C320000 and C330130) and the National Research Foundation of Korea grants (2023R1A2C1006973 and 2022H1D3A2A02093655).

ABBREVIATIONS

MB, methylene blue; MT^+, methylthioninium; LMT, leuco-methylthioninium; LMTM, leuco-methylthioninium bis-hydromethanesulfonate; tau, tubulin-associated unit; Cys, cysteine; Lys, lysine; HSQC; NMR, nuclear magnetic resonance; DTT, dithiothreitol; DMSO, dimethyl sulfoxide; interDS, intermolecular disulfide bond; CSP, chemical shift perturbation; SEC-MALS, size-exclusion chromatography-multiangle light scatter-

ing; CS, chemical shift; NAC, *N*-acetylcysteine; E_a, activation energy

REFERENCES

(1) Jadhav, S.; Avila, J.; Scholl, M.; Kovacs, G. G.; Kovari, E.; Skrabana, R.; Evans, L. D.; Kontsekova, E.; Malawska, B.; de Silva, R.; et al. A walk through tau therapeutic strategies. *Acta Neuropathol Commun.* **2019**, *7* (1), 22.

(2) Wischik, C. M.; Schelter, B. O.; Wischik, D. J.; Storey, J. M. D.; Harrington, C. R. Modeling Prion-Like Processing of Tau Protein in Alzheimer's Disease for Pharmaceutical Development. *J. Alzheimers Dis* **2018**, *62* (3), 1287−1303.

(3) Clifton, J., 2nd; Leikin, J. B. Methylene blue. *Am. J. Ther* **2003**, *10* (4), 289−291.

(4) Baddeley, T. C.; McCaffrey, J.; Storey, J. M.; Cheung, J. K.; Melis, V.; Horsley, D.; Harrington, C. R.; Wischik, C. M. Complex disposition of methylthioninium redox forms determines efficacy in tau aggregation inhibitor therapy for Alzheimer's disease. *J. Pharmacol Exp Ther* **2015**, *352* (1), 110−118.

(5) Jouanne, M.; Rault, S.; Voisin-Chiret, A. S. Tau protein aggregation in Alzheimer's disease: An attractive target for the development of novel therapeutic agents. *Eur. J. Med. Chem.* **2017**, *139*, 153−167.

(6) Akoury, E.; Pickhardt, M.; Gajda, M.; Biernat, J.; Mandelkow, E.; Zweckstetter, M. Mechanistic basis of phenothiazine-driven inhibition of Tau aggregation. *Angew. Chem., Int. Ed. Engl.* **2013**, *52* (12), 3511−3515.

(7) Kiss, R.; Csizmadia, G.; Solti, K.; Keresztes, A.; Zhu, M.; Pickhardt, M.; Mandelkow, E.; Toth, G. Structural Basis of Small Molecule Targetability of Monomeric Tau Protein. *ACS Chem. Neurosci.* **2018**, *9* (12), 2997−3006.

(8) La Rocca, R.; Tsvetkov, P. O.; Golovin, A. V.; Allegro, D.; Barbier, P.; Malesinski, S.; Guerlesquin, F.; Devred, F. Identification of the three zinc-binding sites on tau protein. *Int. J. Biol. Macromol.* **2022**, *209* (Pt A), 779−784.

(9) Gallivan, J. P.; Dougherty, D. A. Cation-pi interactions in structural biology. *Proc. Natl. Acad. Sci. U. S. A.* **1999**, *96* (17), 9459−9464.

(10) Crowe, A.; James, M. J.; Lee, V. M.; Smith, A. B., 3rd; Trojanowski, J. Q.; Ballatore, C.; Brunden, K. R. Aminothienopyridazines and methylene blue affect Tau fibrillization via cysteine oxidation. *J. Biol. Chem.* **2013**, *288* (16), 11024−11037.

(11) Kelner, M. J.; Alexander, N. M. Methylene blue directly oxidizes glutathione without the intermediate formation of hydrogen peroxide. *J. Biol. Chem.* **1985**, *260* (28), 15168−15171.

(12) Benson, B. B.; Krause, J. D. The concentration and isotopic fractionation of oxygen dissolved in freshwater and seawater in equilibrium with the atmosphere. *Limnol Oceanogr* **1984**, *29* (3), 620−632.

(13) Limpanuparb, T.; Roongruangsree, P.; Areekul, C. A DFT investigation of the blue bottle experiment: E(composite function)-(half-cell) analysis of autoxidation catalysed by redox indicators. *R Soc. Open Sci.* **2017**, *4* (11), No. 170708.

(14) Al-Hilaly, Y. K.; Pollack, S. J.; Rickard, J. E.; Simpson, M.; Raulin, A. C.; Baddeley, T.; Schellenberger, P.; Storey, J. M. D.; Harrington, C. R.; Wischik, C. M.; et al. Cysteine-Independent Inhibition of Alzheimer's Disease-like Paired Helical Filament Assembly by Leuco-Methylthioninium (LMT). *J. Mol. Biol.* **2018**, *430* (21), 4119−4131.

(15) Fitzpatrick, A. W. P.; Falcon, B.; He, S.; Murzin, A. G.; Murshudov, G.; Garringer, H. J.; Crowther, R. A.; Ghetti, B.; Goedert, M.; Scheres, S. H. W. Cryo-EM structures of tau filaments from Alzheimer's disease. *Nature* **2017**, *547* (7662), 185−190.

(16) Weismiller, H. A.; Holub, T. J.; Krzesinski, B. J.; Margittai, M. A thiol-based intramolecular redox switch in four-repeat tau controls fibril assembly and disassembly. *J. Biol. Chem.* **2021**, *297* (3), No. 101021.

(17) Oz, M.; Lorke, D. E.; Hasan, M.; Petroianu, G. A. Cellular and molecular actions of Methylene Blue in the nervous system. *Med. Res. Rev.* **2011**, *31* (1), 93−117.

(18) McKeown, S. R. Defining normoxia, physoxia and hypoxia in tumours-implications for treatment response. *Br J. Radiol* **2014**, *87* (1035), No. 20130676.

(19) Riha, P. D.; Bruchey, A. K.; Echevarria, D. J.; Gonzalez-Lima, F. Memory facilitation by methylene blue: dose-dependent effect on behavior and brain oxygen consumption. *Eur. J. Pharmacol.* **2005**, *511* (2−3), 151−158.

https://doi.org/10.1021/jacsau.4c00262
JACS Au 2024, 4, 2451−2455